Supplementary Material

Trait-based mechanisms underpin regional hotspot of diatom-driven carbon export in an oligotrophic gyre

Feng Li[1#], Hongzhen Jiang[1#], Linwei Liu[1], Zhouyi Jiang[1], Lu Huang[1], kehui Feng[1], Zuozhu Wen[2], Xin Liu[2], Changping Chen[1], Kuanbo Zhou[2*], Junrong Liang[1*]

[1]School of Life Sciences, Key Laboratory of Ministry of Education for Coastal and Wetland Ecosystems, Xiamen Key Laboratory of Plant Genetics, Xiamen University, Xiamen 361102, Fujian, China.

[2]College of Ocean and Earth Sciences, State Key Laboratory of Marine Environment Science, Xiamen University, Xiamen 361102, Fujian, China.

#These authors contributed equally to this work.

*Corresponding author: sunljr@xmu.edu.cn (Junrong Liang); kbzhou@xmu.edu.cn (Kuanbo Zhou)

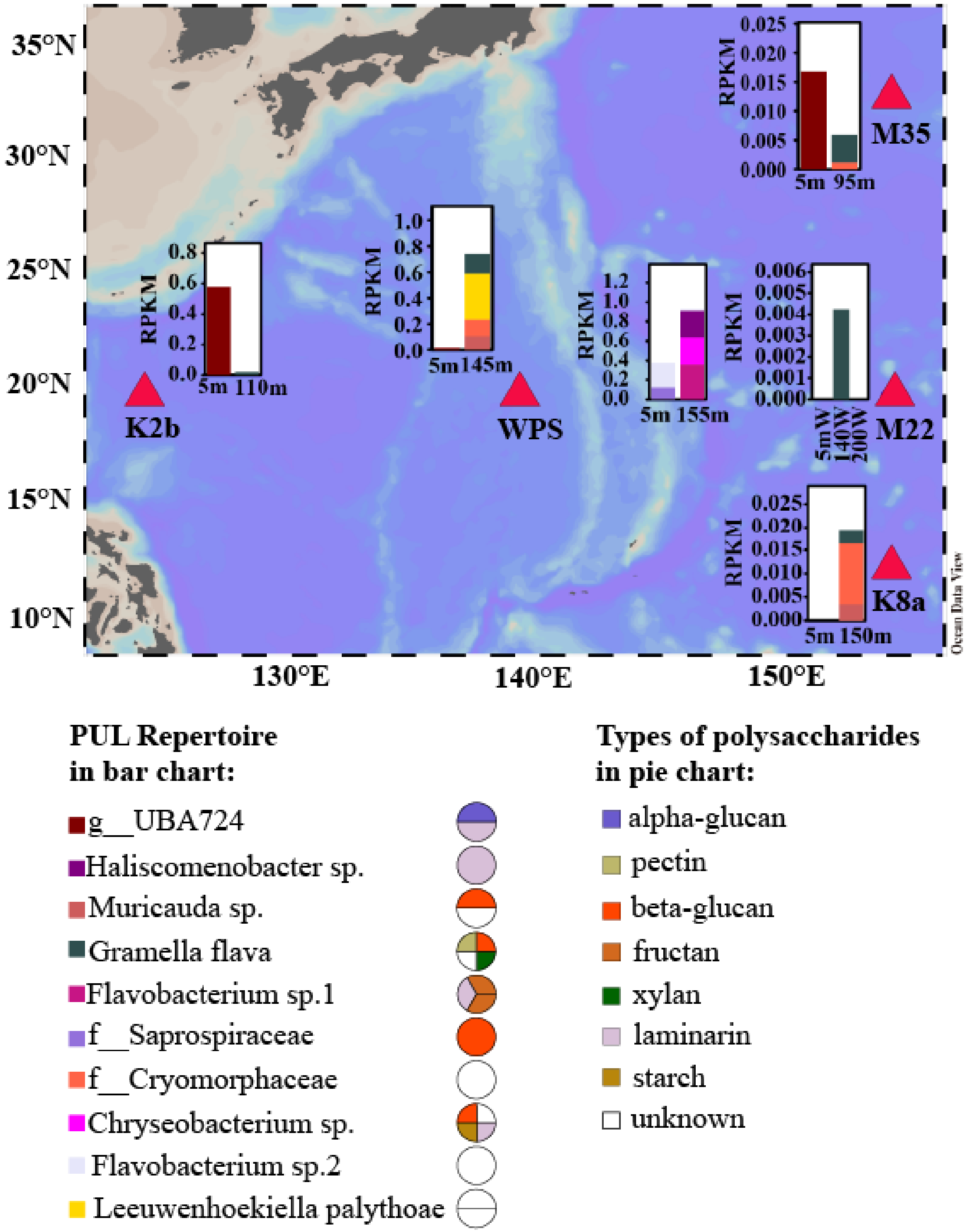

Fig. S1 Abundance pattern of Bacteroidetes MAGs with PUL annotations. In all bar charts, MAG abundance is represented by RPKM. The pie chart partitions reflect the quantity of PULs possessed by the bacteria, with colors corresponding to the types of polysaccharides that may be degraded. MAGs, metagenome-assembled genomes. PUL, polysaccharide utilization loci.

Table S1 Overview of sampled stations, collected methods, and sample details

Sample type	Station	The depth of sampling (m)			Sampling methods
Water samples (summer)	K2b	5	DCM (110)	200	CTD
	WPS	5	DCM (145)	200	
	M22	5	DCM (155)	200	
	K8a	5	DCM (150)	200	
	M35	5	DCM (95)	200	
Water samples (winter)	M22	5	DCM (135)	200	CTD
	K8a	5	DCM (146)	200	
Sediment trap samples (summer)	K2b	50	100	200	Sediment trap
	M22	50	100	200	
	K8a	50	100	200	
Environmental DNA samples(summer)	K2b	5	DCM (110)	-	In-situ large-volume filter pumps
	WPS	5	DCM (145)	-	
	M22	5	DCM (155)	-	
	K8a	5	DCM (150)	-	
	M35	5	DCM (95)	-	

Environmental DNA samples(winter)	M22	5	DCM (135)	200	In-situ large-volume filter pumps

Note: “-” indicates unavailable samples.

The depth of sampling refers to the collection of samples from three distinct depths: 5 m, the depth of the deep chlorophyll maximum (DCM), 200 m. For sediment trap samples, the three distinct depths are 50m, 100m, and 200m, respectively.

Table S2 Estimation of average carbon biomass values for diatom genera and species

Genus or species	Carbon content (pg C cell^{-1})	The source of the data
Thalassiothrix	422	Harrison et al., 2015
Thalassiosira	848.3	Harrison et al., 2015
Thalassiosira pacifica	848.3	Harrison et al., 2015
Thalassionema	84.7	Harrison et al., 2015
Thalassionema nitzschioides	63.4	Harrison et al., 2015
Thalassionema frauenfeldii	106	Harrison et al., 2015
Synedra	2176.6	Measurement and calculation
Rhizosolenia	2064	Harrison et al., 2015
Rhizosolenia styliformis	3560	Harrison et al., 2015
Rhizosolenia imbricata	1620	Harrison et al., 2015
Rhizosolenia hyalina	2064	Harrison et al., 2015
Rhizosolenia clevei	2064	Harrison et al., 2015
Pseudo-nitzschia pungens	86.9	Harrison et al., 2015
Protoraphis	19.1	Measurement and calculation
Pleurosigma	1580.6	Chitari et al., 2017
Planktoniella	8351.2	Chitari et al., 2017
Planktoniella formosa	8351.2	Chitari et al., 2018
Pinnularia	590	Rath et al., 2023
Nitzschia	36.9	Harrison et al., 2015
Nitzschia lorenziana	36.9	Harrison et al., 2015
Nitzschia longissima	43.4	Harrison et al., 2015
Navicula	107.1	Calculation
Mastogloia rostrata	265.5	Measurement and calculation
Leptocylindrus danicus	123	Harrison et al., 2015
Hemiaulus	728.5	Harrison et al., 2015

Hemiaulus hauckii	533	Harrison et al., 2015
Haslea	199.5	Measurement and calculation
Guinardia striata	1290	Harrison et al., 2015
Guinardia flaccida	4870	Harrison et al., 2015
Eunotogramma	44.49	Measurement and calculation
Eucampia	441	Harrison et al., 2015
Eucampia zodiacus	441	Harrison et al., 2015
Eucampia cornuta	441	Harrison et al., 2015
Ditylum brightwelii	2340	Harrison et al., 2015
Coscinodiscus	28411.3	Harrison et al., 2015
Chaetoceros	176.3	Harrison et al., 2015
Chaetoceros pelagicus	176.3	Harrison et al., 2015
Cerataulina pelagica	452	Harrison et al., 2015
Bellerochea horologicalis	1140	Harrison et al., 2015
Bacteriastrum	554.5	Harrison et al., 2015
Asteromphalus	2187.3	Chen et al., 2023; Rath et al., 2023
Asteromphalus Arachne	2187.3	Chen et al., 2023; Rath et al., 2023
Asterolampra	287	Harrison et al., 2015
Asterolampra vanheurckii	287	Harrison et al., 2015
Asterionella	46.2	Harrison et al., 2015
Ampora	65	Rath et al., 2023

Table S3 Proportion of dominant species based on carbon biomass across sampling stations and corresponding depth layers

Dominant species	Carbon biomass and proportion in summer (ng C L^{-1}(%))		
	K2b 5m	K2b DCM	K2b 200m
Rhizosolenia	36.84 (71%)	17.80 (8%)	0.74 (7%)
Thalassiosira	0	29.69 (14%)	0
Nitzschia	0.37 (0.7%)	6.71 (3%)	10.32 (93%)
Navicula	8.03 (15%)	2.14 (1%)	0
Coscinodiscus	0	142.06 (66%)	0
	M22 5m	M22 DCM	M22 200m
Rhizosolenia	29.05 (84%)	0	7.12 (38%)
Thalassiosira	1.70 (5%)	2.54 (4%)	2.54 (13%)
Nitzschia	0.07 (0.2%)	0.63 (1%)	5.90 (31%)
Ditylum brightwelii	0	39.78 (62%)	0
Planktoniella formosa	0	16.70 (26%)	0
	K8a 5m	K8a DCM	K8a 200m
Thalassiosira	8.48 (69%)	12.72(62%)	8.48 (73%)
Nitzschia	0.37 (3%)	2.21 (11%)	1.11 (10%)
Thalassiothrix	0	2.11 (10%)	0
Navicula	0	2.68 (13%)	1.07 (9%)
Hemiaulus	2.66 (22%)	0	0
	WPS 5m	WPS DCM	WPS 200m
Thalassiosira	0	0	8.48 (83.10%)
Nitzschia	0	1.11 (34%)	1.17 (11%)
Navicula	1.61 (78%)	2.14 (66%)	0
Eunotogramma	0.44 (22%)	0	0
	M35 5m	M35 DCM	M35 200m
Nitzschia	6.83 (37%)	9.96 (0.8%)	0.37 (2%)

Navicula	3.75 (20%)	3.21 (0.3%)	0
Coscinodiscus	0	568.22 (46%)	0
Mastogloia rostrata	2.65 (14%)	0	0
Thalassiosira	0	59.38 (5%)	0
Bacteriastrum	0	32.41 (3%)	8.32 (50%)
Chaetoceros	0	156.91 (13%)	0
Eucampia	2.21 (12%)	8.82 (0.7%)	0
Guinardia	0	161.90 (13%)	0
Pinnularia	2.95 (16%)	5.90 (0.5%)	0
Pleurosigma	0	0	7.90 (48%)
Dominant species	Carbon biomass and proportion in winter (ng C L^{-1}(%))		
	M22 5m	M22 DCM	M22 200m
Rhizosolenia	20.64 (28%)	10.32 (38%)	10.32 (50%)
Thalassiosira	8.48 (11%)	4.24 (16%)	0
Nitzschia	0	5.90 (22%)	0
Thalassionema	0	2.96 (11%)	0
Climacodium	34.55 (47%)	0	0
Synedra	0	0	10.88 (53%)
	K8a 5m	K8a DCM	K8a 200m
Rhizosolenia	20.64 (39%)	0	0
Thalassiosira	12.72 (24%)	4.24 (24%)	4.24 (41%)
Nitzschia	0	7.93 (45%)	2.95 (28%)
Thalassiothrix	0	2.11 (12%)	2.11 (20%)

Table S4 Alpha diversity index of the diatom community based on carbon biomass in summer

Sample sites	Richness	Pielou	Simpson
K2b_5m	6	0.79	0.71
K2b_DCM	9	0.53	0.53
K2b_200m	2	0.35	0.12
WPS_5m	2	0.75	0.34
WPS_DCM	2	0.93	0.45
WPS_200m	4	0.46	0.30
M22_5m	11	0.44	0.46
M22_DCM	10	0.47	0.55
M22_200m	9	0.71	0.73
K8a_5m	5	0.57	0.48
K8a_DCM	5	0.73	0.58
K8a_200m	6	0.81	0.71
M35_5m	6	0.87	0.77
M35_DCM	19	0.65	0.75
M35_200m	4	0.58	0.52

Table S5 Alpha diversity index of the diatom community based on carbon biomass in winter

Sample sites	Richness	Pielou	Simpson
M22_5m	7	0.66	0.65
M22_DCM	7	0.84	0.76
M22_200m	4	0.61	0.53
K8a_5m	10	0.78	0.77
K8a_DCM	6	0.82	0.71
K8a_200m	6	0.78	0.71

Table S6 Dominant species, based on cell abundance, contributing to export Flux

Dominant species of each station	Flux of intact cells (cells m^{-2} d^{-1})		
	K2b 50m	K2b 100m	K2b 200m
Rhizosolenia spp.	83227	3567	18004
Nitzschia spp.	49257	6964	17325
Mastogloia rostrata	57749	3057	12909
Bellerochea horologicalis	0	0	5775
Thalassionema nitzschioides	0	1189	3397
	M22 50m	M22 100m	M22 200m
Nitzschia spp.	15966	17495	8832
Thalassionema nitzschioides	340	1868	849
Navicula spp.	7304	1359	679
Thalassiosira spp.	0	0	170
Pinnularia sp.	170	510	170
	K8a 50m	K8a 100m	K8a 200m
Nitzschia spp.	679	510	3907
Navicula spp.	170	170	2378
Thalassiosira spp.	0	510	849
Mastogloia rostrata	340	0	340
Thalassionema spp.	0	0	340

Table S7 The contribution of diatom carbon production to total phytoplankton carbon production in the water column

Station	Depth	Carbon content of diatoms (ng C L^{-1})	Carbon content of total phytoplankton (mg C L^{-1})	The percentage of diatom carbon in total phytoplankton carbon (%)
K2b	5	52.2	4.24	1.2
K2b	DCM (110m)	213.9	3.14	6.8
K2b	200	11.1	3.54	0.3
M22	5	34.5	2.38	1.5
M22	DCM (155m)	64.4	3.14	2.0
M22	200	18.9	1.59	1.2
K8a	5	12.3	1.13	1.1
K8a	DCM (150m)	20.6	3.10	0.7
K8a	200	11.6	0.92	1.3

Table S8 The contribution of diatom carbon export to total phytoplankton carbon export

Station	Depth	Carbon content of diatoms (mg C $m^{-2}d^{-1}$)	Carbon content of total phytoplankton (mg C m^{-2} d^{-1})	The percentage of diatom carbon in total phytoplankton carbon (%)
K2b	50	194.85	0.97	20.0
K2b	100	8.87	0.05	16.6
K2b	200	52.4	0.30	17.2
M22	50	3.76	0.28	1.3
M22	100	9.12	0.11	8.4
M22	200	0.79	0.10	0.8
K8a	50	0.13	0.66	0.02

K8a	100	0.52	0.09	0.6
K8a	200	2.42	0.18	1.4

Table S9 Comparison of diatom abundance across different oceans

Study area	Times	Depth (m)	diatom abundance (cell/L)	Range	Reference	Nutriture
the western South China Sea	2007.08-09	0-200	827	10°-15° N 110°-112.5° E	Ding et al., 2021	oligotrophic
the tropical Eastern Indian Ocean	2019.03-05	5-150	19 ± 10	10°S-14°N 80°E-94°E	Wei et al., 2021	oligotrophic
the South Atlantic Ocean	2013.03-05	5	$2\text{-}21\times 10^{3}$	10°N-38° S 20°-60° W	Durkin et al., 2016	oligotrophic
Kuroshio region	2011.01-02	0	139-696	31.03°-33.6°N 140°-145°E	Girault et al., 2016	oligotrophic
Pacific subtropical gyre	2011.01-02	0, SCM	16-300	22.83°-28.98°N 140°-145°E	Girault et al., 2016	oligotrophic
Transition zone	2011.01-02	0	5-32	13.25-20.78°N 140°-145°E	Girault et al., 2016	oligotrophic
Warm Pool	2011.01-02	0	19-271	13.27°S-9.19°N 140°-160°E	Girault et al., 2016	oligotrophic
Taiwan Strait	2019.07	Surface (up to 1 m depth)	3640-166,000	24.95°-26.35°N 119.38°-120.57° E	Zhang et al., 2020	nutritionally adequate

northern South China Sea	2012.07-08	5-200	1.954×10^{3}	18°-22°N 110°-116°E	Wei et al., 2018	nutritionally adequate
the southern Yellow Sea	2008.07	Surface-bottom	26.7×10^{3}	33.5°-36.0°N 120.5°-123.0°E	Yang & Liu, 2018	nutritionally adequate
Panighat in the coastal waters of south Andaman Sea, India	2013.03-10	Surface	12.31×10^{5}	11.5°-12.25°N 92.5°-92.75°E	Manjumol et al., 2018	nutritionally adequate
Western North Pacific	2020.07-08	0-200	235	10°- 35°N 120°-160°E	This study	oligotrophic

Table S10 Comparison of diatom flux across different oceans

Study area	Times	Depth(m)	diatom flux (cells m^{-2} d^{-1})	Range	Reference	Nutriture
the South Atlantic Ocean	2013.03-05	5	$0.037–0.627 \times 10^{6}$	10°N-38° S 20°-60° W	Durkin et al., 2016	Oligotrophic
the western equatorial Atlantic (WA3)	1994.01.21-1994.02.14	671	0.9×10^{5}	7.51°S 28.03°W	Romero et al., 2000	Oligotrophic
the oligotrophic North Pacific gyre (ALOHA)	1994.07.22	165	ca. 9.4×10^{6}	22.75°N 158°W	Scharek et al., 1999	Oligotrophic
the oligotrophic North Pacific gyre (ALOHA)	1994.08.28	165	ca. 2.6×10^{6}	22.75°N 158°W	Scharek et al., 1999	Oligotrophic
the oligotrophic North Pacific gyre (ALOHA)	1995.07.28	165	ca. 1.3×10^{6}	22.75°N 158°W	Scharek et al., 1999	Oligotrophic
the subtropical northeastern Atlantic （Mauritania）	1988.03-2009.06	1246-3633	Average 4.0×10^{5}	20.76°-21.29°N 19.74°-20.85°W	Romero et al., 2021	nutritionally adequate
the Southern Ocean (KERFIX station)	1994.07.31-1994.8.31	280	1×10^{6}	50.67° S 68.42°E	Rembauville et al., 2018	HNLC

the Southern Ocean (The Subantarctic Zone (SAZ))	2003-2004	500	8.1 $\times 10^5$	46.77° S 142.07° E	Wilks et al., 2017	HNLC
Western North Pacific	2020.07-08	0-200	（0.2-39.6）$\times 10^4$	10°- 35°N 120°-160°E	This study	Oligotrophic

References

1) Chen, D., Z. Shi, R. Li, X. Li, Y. Cheng, and J. Xu. 2023. Hydrodynamics drives shifts in phytoplankton community composition and carbon-to-chlorophyll a ratio in the northern South China Sea. Frontiers in Marine Science 10. https://doi.org/10.3389/fmars.2023.1293354.
2) Ding, C. L., J. Sun, D. D. Narale, and H. J. Liu. 2021. Phytoplankton Community in the Western South China Sea in Winter and Summer. Water **13**. doi:https://doi.org/10.3390/w13091209
3) Durkin, C. A., B. A. S. Van Mooy, S. T. Dyhrman, and K. O. Buesseler. 2016. Sinking phytoplankton associated with carbon flux in the Atlantic Ocean. Limnol. Oceanogr. **61**: 1172-1187. doi:https://doi.org/10.1002/lno.10253
4) Girault, M., G. Gregori, A. Barani, and H. Arakawa. 2016. A study of microphytoplankton and cyanobacteria consortia in four oligotrophic regimes in the western part of the North Pacific subtropical gyre and in the warm pool. J. Plankton Res. **38**: 1317-1333. doi:https://doi.org/10.1093/plankt/fbw056
5) Harrison, P. J. and others. 2015. Cell volumes of marine phytoplankton from globally distributed coastal data sets. Estuarine Coastal and Shelf Science 162: 130-142. https://doi.org/10.1016/j.ecss.2015.05.026.
6) Manjumol, C. C., C. L. Libini, K. A. A. Idu, K. S. Mohamed, and V. Kripa. 2018. Occurrence of Diatom - Diazotrophic association in the coastal surface waters of south Andaman, India. Symbiosis **76**: 293-302. doi:https://doi.org/10.1007/s13199-018-0559-y
7) Rath, A. R., S. Mitbavkar. 2023. Diatom community dynamics in a tropical brackish coastal ecosystem from an ecological and biogeochemical perspective: A size-fractionated approach. Continental Shelf Research 263: 105039. https://doi.org/10.1016/j.csr.2023.105039.
8) Rembauville, M., I. Salter, F. Dehairs, J. C. Miquel, and S. Blain. 2018. Annual particulate matter and diatom export in a high nutrient, low chlorophyll area of the Southern Ocean. Polar Biol. **41**: 25-40. doi:https://doi.org/10.1007/s00300-017-2167-3
9) Romero, O. E., G. Fischer, C. B. Lange, and G. Wefer. 2000. Siliceous phytoplankton of the western equatorial Atlantic: sediment traps and surface sediments. Deep-Sea Research Part II-Topical Studies in Oceanography **47**: 1939-

1959. doi:https://doi.org/10.1016/S0967-0645(00)00012-6

10) Romero, O. E., S. Ramondenc, and G. Fischer. 2021. A 2-decade (1988-2009) record of diatom fluxes in the Mauritanian coastal upwelling: impact of low-frequency forcing and a two-step shift in the species composition. Biogeosciences **18**: 1873-1891. doi:https://doi.org/10.5194/bg-18-1873-2021

11) Scharek, R., M. Latasa, D. M. Karl, and R. R. Bidigare. 1999. Temporal variations in diatom abundance and downward vertical flux in the oligotrophic North Pacific gyre. Deep-Sea Research Part I-Oceanographic Research Papers **46**: 1051-1075. doi:https://doi.org/10.1016/S0967-0637(98)00102-2

12) Wei, N., T. Satheeswaran, I. R. Jenkinsone, B. Xue, Y. Q. Wei, H. J. Liu, and J. Sun. 2018. Factors driving the spatiotemporal variability in phytoplankton in the Northern South China Sea. Cont. Shelf Res. **162**: 48-55. doi:https://doi.org/10.1016/j.csr.2018.04.009

13) Wei, Y. Q., X. Z. Wang, J. Gui, and J. Sun. 2021. Significant Pico- and Nanoplankton Contributions to Biogenic Silica Standing Stocks and Production Rates in the Oligotrophic Eastern Indian Ocean. Ecosystems **24**: 1654-1669. doi:https://doi.org/10.1007/s10021-021-00608-w

14) Wilks, J. V., A. S. Rigual-Hernández, T. W. Trull, S. G. Bray, J. A. Flores, and L. K. Armand. 2017. Biogeochemical flux and phytoplankton succession: A year-long sediment trap record in the Australian sector of the Subantarctic Zone. Deep-Sea Research Part I-Oceanographic Research Papers **121**: 143-159. doi:https://doi.org/10.1016/j.dsr.2017.01.001

15) Yang, S. M., and X. S. Liu. 2018. Characteristics of phytoplankton assemblages in the southern Yellow Sea, China. Mar. Pollut. Bull. **135**: 562-568. doi:https://doi.org/10.1016/j.marpolbul.2018.07.062

16) Zhang, Y., J. Z. Su, Y. P. Su, H. Lin, Y. C. Xu, B. P. Barathan, W. N. Zheng, and K. G. Schulz. 2020. Spatial Distribution of Phytoplankton Community Composition and Their Correlations with Environmental Drivers in Taiwan Strait of Southeast China. Diversity-Basel **12**: 433. doi:https://doi.org/10.3390/d12110433